

Probing the primordial power spectra with inflationary priors

Masahiro Kawasaki^{1,2}, Toyokazu Sekiguchi¹

¹*Institute for Cosmic Ray Research, University of Tokyo, Kashiwa 277-8582, Japan*

²*Institute for the Physics and Mathematics of the Universe, University of Tokyo, Kashiwa, Chiba, 277-8568, Japan*

Abstract

We investigate constraints on power spectra of the primordial curvature and tensor perturbations with priors based on single-field slow-roll inflation models. We stochastically draw the Hubble slow-roll parameters and generate the primordial power spectra using the inflationary flow equations. Using data from recent observations of CMB and several measurements of geometrical distances in the late Universe, Bayesian parameter estimation and model selection are performed for models that have separate priors on the slow-roll parameters. The same analysis is also performed adopting the standard parameterization of the primordial power spectra. We confirmed that the scale-invariant Harrison-Zel'dovich spectrum is disfavored with increased significance from previous studies. While current observations appear to be optimally modeled with some simple models of single-field slow-roll inflation, data is not enough constraining to distinguish these models.

1 Introduction

Cosmological observations, including the cosmic microwave background (CMB), large scale structure, baryon acoustic oscillation (BAO), type Ia supernovae (SN) offer opportunities to probe a number of physics far beyond the reach of experiments in terrestrial laboratories. Among such physics is inflation, that solves various problems in the hot universe scenario [1–5]. In addition, inflation also explains generation of initial perturbations for structure formation [6–13]. Inflation is an essential part of our best description of the Universe.

The simplest class of models of inflation is so-called single-field slow-roll inflation [4, 5], where potential energy of a single scalar field (inflaton), that is slowly varying its field value, drives an exponential expansion of the Universe. Gaussian, nearly scale-invariant primordial curvature perturbation can be generated from the vacuum fluctuation of inflaton in a quasi-de Sitter spacetime. Such primordial perturbation gives excellent fits to various data from cosmological observations, which makes single-field slow-roll inflation highly attractive. However we yet know quite little about inflaton which might actually drive an inflationary epoch in our Universe.

Identification of inflaton is of particular interest both in cosmology and particle physics. As a model of single-field slow-roll inflation largely affects the late Universe in an observable way through generation of the primordial curvature and tensor perturbations, constraints on models have been mainly investigated through constraining power spectra of these primordial perturbations, $\mathcal{P}_\zeta(k)$ and $\mathcal{P}_h(k)$, using various cosmological observations^{#1}. One of the most familiar way may be to adopt the standard parameterization for the power spectra, $A_s, r, n_s, n_t, \alpha_s$, etc. (See Eqs. (15-19)), and derive constraints on these parameters. Some more involved analyses have also been performed focusing on reconstruction of the potential of the inflaton or slow-roll flow parameters [14–31]. In either way, deviation from the Harrison-Zel’dovich (HZ) spectrum (i.e. $r = 0$ and $n_s = \alpha_s = \dots = 0$) allows us to probe models of single-field slow-roll inflation. Cosmological data now signifies some spectral features in the power spectrum of the curvature perturbation. When we assume a power-law curvature perturbation spectrum $\mathcal{P}_\zeta(k) \propto A_s k^{n_s - 1}$ and absence of the tensor perturbation $\mathcal{P}_h(k) = 0$, recent CMB data from WMAP give $-0.065 < n_s - 1 < -0.009$ (95% C.L.), suggesting a significant deviation from the HZ power spectrum [32].

However, constraints on the primordial power spectra are highly dependent of parameter spaces where we investigate constraints. In fact, if running of the spectral index is included in the parameter estimation, the HZ spectrum is in turn allowed at 95% C.L. [32].

Therefore, since we do not in advance know a parameter space where we should explore a constraint on the power spectra, we also need to consider if the parameter space is appropriate. More generally, appropriateness of a model, which possesses its own prior assumption, should also discussed. A guiding principle in looking for an optimal model is Occam’s razor, which penalizes unnecessary assumption in describing observations. Bayesian model selection is Bayesian implementation of Occam’s razor, which is now frequently applied

^{#1} There are also several other probes for inflation models, including primordial isocurvature perturbations and non-Gaussianity in primordial perturbations.

in the context of cosmology [33–51]. Indeed, authors in Ref. [24] have adopted Bayesian model selection to assess optimal orders up to which reconstruction of inflaton potential should be performed.

Motivated by [24] and other earlier studies, we investigate an optimal constraint on primordial perturbation spectra and comparison of single-field slow-roll inflation models using recent cosmological observations, which would be a subject of great interest [52]. Bayesian model selection is applied more vigorously. We compare Bayes evidences for several models which have separate priors on inflationary slow-roll parameters, or parameters for primordial power spectra. Each of these models represents some class of single-field slow-roll inflation models. In this paper we implicitly assume a Freedman-Robertson-Walker universe and adopt natural units $\hbar = c = M_{\text{Pl}} = 1$.

This paper is organized as follows: In Section 2 we briefly review the Hubble slow-roll flow equations, which are adopted in our analysis. Then in Section 3, some essences of Bayesian model selection are also reviewed. The main part of our paper is Section 4, where we investigate constraints on the primordial power spectra using data from recent observations of CMB and geometrical distances in the late Universe. By employing Bayesian model selection, an optimal constraint and comparison of models of single-field slow-roll inflation are investigated. The final section is devoted to summary and future outlook.

2 Hubble slow-roll flow equations

We make use of the *Hubble slow-roll* (HSR) flow equations [16, 19, 53], that reside in more general inflationary flow equations [54, 55]. Here we give some key consequences of the HSR formalism. In this paper, we assume models of single-field slow-roll inflation have canonical kinetic terms and do not investigate non-canonical models.

During an epoch of slow-roll inflation, the inflaton field ϕ can be safely assumed as a monotonic function of the time and hence regarded as a generalized time coordinate. Instead of solving the Hamilton-Jacobi equation [55] for given inflaton potential, we rather solve a set of the HSR flow equations given by

$$\epsilon_H(\phi) = \frac{1}{4\pi} \left(\frac{H(\phi)'}{H(\phi)} \right)^2, \quad (1)$$

$${}^\ell \lambda_H(\phi) = \left(\frac{1}{4\pi} \right)^\ell \frac{(H(\phi)')^{\ell-1} d^{\ell+1} H(\phi)}{H(\phi)^\ell d\phi^{\ell+1}} \quad (\text{for } \ell \geq 1). \quad (2)$$

Here and hereafter we denote derivatives respective to ϕ as prime (e.g. $H' \equiv dH/d\phi$). These flow equations are solved once we specify the initial values for ϵ_H and ${}^\ell \lambda_H$ at a fiducial ϕ_* ,

$$\epsilon_{H*} \equiv \epsilon_H(\phi_*), \quad (3)$$

$${}^\ell \lambda_{H*} \equiv {}^\ell \lambda_H(\phi_*) \quad (\text{for } \ell \geq 1). \quad (4)$$

If we choose fiducial HSR parameters ${}^\ell\lambda_{H_*} = 0$ for $\ell > M$, the HSR parameters ${}^\ell\lambda_H(\phi)$ for $\ell > M$ also vanish at any ϕ and hence the flow equations are truncated at order M . In this case, the Hubble expansion rate can be exactly solved [56]. Without loss of generality, we can choose $\phi_* = 0$ and ϕ being a decreasing function of time (i.e. $H'(\phi) > 0$). Then we obtain

$$H(\phi) = H_*(1 + B_1\phi + B_2\phi^2 + \dots + B_{M+1}\phi^{M+1}), \quad (5)$$

where $H_* = H(\phi_*)$ and the coefficients of the Taylor expansion, B_i ($i = 1, \dots, M+1$), are given by the HSR parameters at the fiducial point,

$$B_1 = \sqrt{4\pi \epsilon_{H_*}}, \quad (6)$$

$$B_{\ell+1} = \frac{(4\pi)^\ell}{(\ell+1)!B_1^{\ell-1}} {}^\ell\lambda_{H_*} \quad (\text{for } \ell \geq 1). \quad (7)$$

Since we have specified the function $H(\phi)$, we already know the dynamics of the background universe and related variables as functions of ϕ . For example, e-folding number $N(\phi)$ at time ϕ is given by integrating

$$\frac{dN}{d\phi} = -\sqrt{\frac{4\pi}{\epsilon_H(\phi)}}. \quad (8)$$

Similarly, a wave number that exits the horizon at time ϕ is given by integrating

$$\frac{d \ln k}{d\phi} = -\sqrt{\frac{4\pi}{\epsilon_H(\phi)}}(1 - \epsilon_H(\phi)). \quad (9)$$

Once we fix a fiducial wave number $k_* = k(\phi_*)$, there is a one-to-one correspondence in k and ϕ by Eq. (9), as long as slow-rolling of the inflaton does not break down. Then any other function of ϕ is rewritten as that of k . For later convenience, we choose the e-folding number $N(k)$ so that it vanishes at a wave number $k = 10^{-4}\text{Mpc}^{-1}$, which roughly corresponds to the scale of current horizon $\simeq 10$ Gpc.

In this paper, we truncate the HSR flow equations at $M = 2$. This is because higher order HSR parameters may not be important due to the limited range of observable wave numbers $\mathcal{O}(10^{-4}) < k < \mathcal{O}(0.1) \text{Mpc}^{-1}$ and accuracy of data at present or in the near future. The fiducial HSR parameters up to $M = 2$ are nothing but the usual slow-roll parameters $\epsilon(\phi)$, $\eta(\phi)$ and $\xi(\phi)$, that are given by

$$\epsilon(\phi) = \epsilon_H(\phi), \quad (10)$$

$$\eta(\phi) = {}^1\lambda_H(\phi), \quad (11)$$

$$\xi(\phi) = {}^2\lambda_H(\phi). \quad (12)$$

One of the most important prediction of single-field inflation models is that the primordial curvature and tensor perturbations are not independent but related to each other

since both are generated from the dynamics of the single scalar field ϕ . In a general meaning, this is the consistency relation for single-field inflation models. At second order in slow-roll approximation, the power spectrum of the primordial curvature and tensor perturbations, $\mathcal{P}_\zeta(k)$ and $\mathcal{P}_h(k)$, respectively, are given by [57]

$$\mathcal{P}_\zeta(k) = \frac{[1 - (2C + 1)\epsilon(\phi) + C\eta(\phi)]^2}{\pi\epsilon(\phi)} H(\phi)^2 \Big|_{\phi=\phi(k)}, \quad (13)$$

$$\mathcal{P}_h(k) = \frac{16[1 - (C + 1)\epsilon(\phi)]^2}{\pi} H(\phi)^2 \Big|_{\phi=\phi(k)}, \quad (14)$$

where $C = -2 + \ln 2 + \gamma \approx -0.729637$ and γ is the Euler constant. Although Eqs. (13-14) are originally derived assuming ϵ and η are constants [57], evolution of these variables are practically very small at observable scales k , which validates the use of Eqs. (13-14)^{#2}.

The standard parameters for the primordial power spectra are given by Taylor expanding the logarithm of Eqs. (13-14),

$$A_s \equiv P_\zeta(k_*), \quad (15)$$

$$n_s \equiv \frac{d \ln \mathcal{P}_\zeta}{d \ln k} \Big|_{k=k_*} + 1 = 1 + 2\eta_* - 4\epsilon_* - 2(1 + C)\epsilon_*^2 - \frac{3 - 5C}{2}\epsilon_*\eta_* + \frac{3 - C}{2}\xi_*, \quad (16)$$

$$r \equiv \frac{P_h}{P_\zeta} \Big|_{k=k_*} = 16\epsilon_*(1 + 2C(\epsilon_* - \eta_*)), \quad (17)$$

$$\alpha_s \equiv \frac{d^2 \ln \mathcal{P}_\zeta}{d \ln k^2} \Big|_{k=k_*} = -2\xi_* - 8\epsilon_*^2 + 10\epsilon_*\eta_*, \quad (18)$$

$$n_t \equiv \frac{d \ln \mathcal{P}_h}{d \ln k} \Big|_{k=k_*} = -2\epsilon_* - (3 + C)\epsilon_*^2 + (1 + C)\epsilon_*\eta_*, \quad (19)$$

where $C = 4(\ln 2 + \gamma) - 5$. With these standard parameters, we can approximate the power spectra by

$$\mathcal{P}_\zeta(k) = A_s \exp \left[(n_s - 1) \ln \frac{k}{k_*} + \frac{1}{2} \alpha_s \left(\ln \frac{k}{k_*} \right)^2 \right], \quad (20)$$

$$\mathcal{P}_h(k) = r A_s \exp \left[n_t \ln \frac{k}{k_*} \right]. \quad (21)$$

Along with the power spectra in Eqs. (13-14), the duration of the inflation is also important. We impose a prior on the e-folding number, $N > 25$. This prior roughly

^{#2} In [28], authors argue effects of differences in the power spectra calculated from exact solution of the wave equation, approximation with slow-roll parameters up to the 2nd order (i.e. Eqs. (13-14)), and more crude approximation with standard parameterization (i.e. Eqs. (20-21)). They conclude that differences among the exact and these approximated power spectra are not significant with a certain prior on the e-folding number N .

means that the energy scale of inflation should be higher than TeV [23]. Imposition of this prior ensures that inflaton does not affect physics below electroweak scales. However, this does not necessarily mean that a given model of single-field slow-roll inflation with certain $(\epsilon_*, \eta_*, \xi_*)$ is excluded if it predicts $N < 25$, for slow-roll parameters at higher orders can maintain slow-rolling of the inflaton further, or even a second inflation can take place. Thus we cannot strictly restrict models of single-field slow-roll inflation with a prior $N > 25$. In Section 4, as default, we adopt a prior $N > 25$ in investigating constraints on the primordial power spectra with inflationary priors. However, we also investigate constraints without the prior $N > 25$, which would be informative in discussing what are plausible models supported from data.

3 Bayesian model selection

As we have mentioned in Introduction, we adopt Bayesian model selection in order to compare different models of single-field slow-roll inflation. Before presenting details of our analysis, let us briefly review some essences of Bayesian model selection. We also refer to [45, 46, 48] for more detailed reviews.

Given data, a joint posterior distribution for a model M and its model parameter Θ , $P(\Theta, M|\text{data})$, is given by the hierarchical Bayes theorem,

$$P(\Theta, M|\text{data}) = \frac{P(\text{data}|\Theta, M)P(\Theta|M)P(M)}{P(\text{data})}, \quad (22)$$

where $P(\text{data}|\Theta, M) = \mathcal{L}(\Theta)$ is the likelihood function, $P(\Theta|M)$ is the prior distribution for Θ specified by M , and $P(M)$ is the prior distribution for M . The remaining $P(\text{data})$ is an irrelevant normalization constant. Then the posterior distribution for M , $P(M|\text{data})$ is given by marginalizing $P(\Theta, M|\text{data})$ over the model parameters Θ ,

$$\begin{aligned} P(M|\text{data}) &= \int d\Theta P(\Theta, M|\text{data}) \\ &= \frac{P(M)}{P(\text{data})} \int d\Theta P(\text{data}|\Theta, M)P(\Theta|M). \end{aligned} \quad (23)$$

The final integral in Eq. (23) is called Bayes evidence $E(M)$,

$$E(M) \equiv \int d\Theta P(\text{data}|\Theta, M)P(\Theta|M), \quad (24)$$

which measures marginalized likelihood of the model M . Thus the relative likelihood of different models M_i and M_j is assessed by the ratio of their Bayes evidence,

$$B_{ij} \equiv \ln \frac{E(M_i)}{E(M_j)} \quad (25)$$

which is called Bayes factor. Bayesian model selection is implemented by estimating Bayes factor which measures relative likelihood between two different models. Jeffreys' scale is often adopted to connect numbers and semantics, which states: for $|B_{ij}| < 1$ the evidence is not significant; $1 < |B_{ij}| < 2.5$ significant; $2.5 < |B_{ij}| < 5$ strong; and $5 < |B_{ij}|$ decisive.

In usual parameter estimation, a posterior distribution of parameters for a model M , $P(\Theta|\text{data}, M)$ is investigated. However, our purpose in this paper of comparing different models of inflation is not achieved via $P(\Theta|\text{data}, M)$, where a model M is by definition assumed to be true. This is another way of representing our statement in Introduction, where we have argued different models cannot be compared with a fixed parameter space. Instead, comparison of different models is achieved by the Bayes factors B_{ij} . This is why we adopt the Bayesian model selection in our analysis. By assigning a prior $P(\Theta|M)$ to reflect prediction of a class of single-field inflation models M , the likelihood of M is measured with the Bays evidence $E(M)$ and two different classes can be compared.

On the other hand, we can also explore an optimal constraint on parameters Θ by adopting Bayesian model selection. By comparing different models, which have separate priors on Θ , an optimal constraints can be obtained from a posterior distribution of the parameters for a model $P(\Theta|\text{data}, M)$ which has higher Bayes evidence than other models.

One remark should be mentioned. The Bayes evidence explicitly depends on a prior probability $P(\Theta|M)$ due to its normalization. For example let us consider that some two different top-hat priors are imposed on a same parameter. Even though the parameter region of high-likelihood is sufficiently covered by both of the priors, the resultant Bayes evidences differs, that are inversely proportional to the ranges of the top-hat priors. This is very contrastive to the usual parameter estimation, where the posterior probabilities from these two different priors do not differ much.

4 Analysis with observational data

Instead of investigating the constraints with priors from various existing models of single-field inflation individually (top-down), we consider several models each of which has its own prior on parameters related to the primordial power spectra (bottom-up). We adopt two parameterizations of the primordial power spectra. One is the standard parameterization that has A_s , n_s , r and α_s . As we are interested in single-field slow-roll inflation models, we impose the standard inflation consistency relation, $n_t = -r/8$, when we adopt the standard parameterization. The other is the HSR parameterization that has A_s , ϵ_* , η_* and ξ_* . By adopting these two parametrizations, models we compare are listed in Table 1. The reference model is M_{HZ} that has the HZ primordial power spectrum. M_{n_s} , $M_{n_s r}$ and $M_{n_s \alpha_s}$ have different top-hat priors on the standard parameters n_s , r and α_s , that are described in the last column of Table 1. On the other hand, M_ϵ , M_η , $M_{\eta\xi}$ have different top-hat priors on the HSR parameters ϵ_* and η_* that are also described in the last column of Table 1. For investigating models with the HSR parameters, we impose an additional prior $N > 25$ as default. Basically, subscripts in a name of a model represent

models	description
M_{HZ}	HZ spectra
M_{n_s}	$0.8 < n_s < 1.2, r = \alpha_s = 0$
$M_{n_s r}$	$0.8 < n_s < 1.2, 0 < r < 0.5, \alpha_s = 0$
$M_{n_s \alpha_s}$	$0.8 < n_s < 1.2, r = 0, -0.1 < \alpha_s < 0.1$
M_ϵ	$0 < \epsilon_* < 0.1, \eta_* = \xi_* = 0$
M_η	$0 < \epsilon_* < 10^{-4}, -0.1 < \eta_* < 0.1, \xi_* = 0$
$M_{\epsilon\eta}$	$0 < \epsilon_* < 0.1, -0.1 < \eta_* < 0.1, \xi_* = 0$

Table 1: Models adopted in the analysis. M_{HZ} is the reference model that has HZ primordial power spectra. Other models cover a model space for single-field slow-roll inflation. M_{n_s} , $M_{n_s r}$, $M_{n_s \alpha_s}$ have top-hat priors on the standard parameters for the primordial power spectra, and M_ϵ , M_η , $M_{\epsilon\eta}$ have ones on the HSR parameters. Prior ranges are described in the last column. Regarding priors on A_s , we adopt a common prior $2.5 < \ln[10^{10} A_s] < 3.5$.

varied parameters in the model, and other parameters absent in the subscripts are fixed to the default values. The only exception is ϵ_* which is varied in a small range $[0, 10^{-4}]$ in M_η ^{#3}. This is because ϵ_* cannot be fixed to zero as the inflaton cannot roll when $\epsilon_* = 0$. Regarding priors on A_s , we adopt a common prior $2.5 < \ln[10^{10} A_s] < 3.5$ in all models. In our analysis a fiducial wave number is chosen to be $k_* = 0.01 \text{ Mpc}^{-1}$ ^{#4}.

We assume a flat Λ CDM model as background cosmology. In addition to parameters representing the shape of the primordial power spectra (i.e. (A_s, n_s, r, α_s) or $(A_s, \epsilon_*, \eta_*, \xi_*)$), following parameters are included in the analysis as primary cosmological parameters,

$$(\omega_b, \omega_c, \theta_s, \tau, A_{SZ}), \quad (26)$$

where ω_b and ω_c are the density parameters of baryon and CDM, respectively, θ_s is the angular scale of the acoustic horizon [59], τ is the optical depth of reionization, and A_{SZ} is the amplitude of template Sunyaev-Zel'dovich power spectrum C_ℓ^{SZ} [60]. The priors on these primary cosmological parameters are listed in Table 2.

We adopt CMB data from WMAP5 [61–63], as well as the observations at small angular scales including ACBAR [64], CBI [65], BOOMERANG [66–68] and QUAD [69]. In addition, we adopt observational data of geometrical distances of the late Universe, including the Union data set of SN [71], the measurement of BAO scales in galaxy power spectra [72]^{#5} and the SH₀ES measurement of the Hubble constant $H_0 = 74.2 \pm 3.6$ [73]. A default data set that we conduct our analysis with is a combination of all the data above,

^{#3} The upper bound 10^{-4} for ϵ_* is chosen so that these models cover inflation scenarios where detection of primordial B-mode would be difficult with CMB observations in the near future.

^{#4} This is very near the recommended value of the fiducial wave number $k_* = 0.017 \text{ Mpc}^{-1}$, which are shown to be optimal for constraining the primordial power spectra from current data [58].

^{#5} We also performed the same analysis by adopting the data of halo power spectra from the catalogue of the SDSS Luminous Red Galaxies [70] instead of the BAO data. However, as long as combined with

parameters	prior ranges
ω_b	[0.02, 0.025]
ω_c	[0.08, 0.14]
θ_s	[1.02, 1.06]
τ	[0.01, 0.2]
A_{SZ}	[0, 4]

Table 2: Top-hat priors on cosmological parameters, other than parameters for the primordial power spectra.

which we denote as ‘ALL’. On the other hand, we also make use of several other data sets, in order to assure ourselves that the results are not dragged by some extreme data. Adopted are data sets of WMAP5 alone and the combinations of WMAP5 with either the other CMB data at small angular scales, BAO, SN, or the H_0 measurement, which we denote as +CMB, +BAO, +SN, + H_0 , respectively.

Computation of Bayes evidences is implemented with `MultiNest` [74], which is integrated in the Markov chain Monte Carlo (MCMC) sampling code `CosmoMC` [75] but uses the nested sampling [76] in stead of the MCMC sampling (See also Ref. [77]). Given a model M , `MultiNest` provides chains of samples from the posterior distribution $P(\Theta|\text{data}, M)$ and a Bayes evidence $E(M)$. Convergence is diagnosed by applying the Gelman-Rubin test with two independent chains. Typically $R - 1 < 0.01$ is achieved.

4.1 Standard parameterization

In Table 3 we listed the Bayes evidences for models with the standard parameters, M_{n_s} , $M_{n_s r}$ and $M_{n_s \alpha_s}$ as well as the reference M_{HZ} from various data sets. There we also listed the Bayes factors for these models against M_{HZ} . From the Table 3, we can first see that current data negatively support the model with the HZ spectrum.

The strongest negative support for M_{HZ} is brought from the ALL data set. Although the Bayes factors depend on alternate models we consider, all models we adopt, M_{n_s} , $M_{n_s r}$ and $M_{n_s \alpha_s}$, give Bayes factors larger than 2.5. On Jeffreys’ scale, these results correspond to strong negative evidences for M_{HZ} . The negative preference for the HZ power spectra has already been reported by many previous studies [35, 37–39, 41, 43] and our result is consistent with the other recent result [47]. Significance in our result is however considerably large as very recent observations are adopted. In Figure 1 we plotted the 1d and 2d marginalized posterior distributions for the parameters n_s , r , and α_s from the

data of CMB, SN and the H_0 measurement, the results are very similar to those from the BAO data. We suppose that this is due to the marginalization over scale-dependent galaxy biases. Although the matter power spectrum themselves is a good probe for the primordial power spectrum at small scales, there are some difficulties in modeling nonlinear evolution of matter perturbations, biases of tracers, or effects of baryonic physics. For the time being, we do not adopt data of the matter power spectrum.

ALL data set. Clearly, the negative support for M_{HZ} originates from a poor fit of the HZ spectrum to the data, as the posterior distributions of n_s for models M_{n_s} , $M_{n_s r}$ and $M_{n_s \alpha_s}$ consistently show a preference for $n_s \neq 1$ of the data.

The Bayes evidences in Table 3 also show that the current data can be well-modeled by a power-law scalar power spectrum without the tensor perturbation (i.e. M_{n_s}). Let us regard M_{n_s} as a base model and ALL as a base data set. When we include the tensor perturbation by varying $r > 0$, the Bayes factors decrease from 4.3 for M_{n_s} to 2.6 for $M_{n_s r}$. This suggests that current data negatively support the presence of the tensor perturbation. In fact, the posterior distribution for r peaks at $r = 0$, as seen in Figure 1. When we include the running of the scalar spectral index, the Bayes factor is almost unchanged from 4.3 for M_{n_s} to 4.4 for $M_{n_s \alpha_s}$. This shows that even though the posterior distribution of α_s in Figure 1 peaks away from $\alpha_s = 0$, the likelihood does not improve much from M_{n_s} in the most region of $\alpha_s \neq 0$ in the $M_{n_s \alpha_s}$ model. We conclude that the presence of α_s is not disfavored by the data nor required in modeling the data.

Similar results are commonly observed with various other combinations of data. From Table 3, the preference for M_{n_s} over $M_{n_s r}$ is commonly observed with all data sets adopted in the analysis. Also M_{n_s} and $M_{n_s \alpha_s}$ are supported almost equally as the Bayesian evidences for these models do not differ by 1 at most. Totally, as M_{n_s} is nested by $M_{n_s r}$ or $M_{n_s \alpha_s}$, we can safely conclude that M_{n_s} models the current data the best among the models with standard parameterization listed in Table 3.

The constraints on cosmological parameters for these models are summarized in Table 4. As we have seen that current data can be optimally modeled by M_{n_s} , we propose the constraint for M_{n_s} as optimal one^{#6}. An optimal constraint on the primordial power spectra from the ALL data set is given by

$$\ln[10^{10} A_s] = 3.137_{-0.032}^{+0.028}, \quad (27)$$

$$n_s = 0.957_{-0.012}^{+0.011}, \quad (28)$$

where errors are given at 68% C.L. Regarding the tensor perturbation and the running of the scalar index, we find no evidence at present.

As a final remark of this section, let us comment on the choice of prior distributions and its relations to the resultant Bayes evidences. As we have mentioned in Section 3, Bayes evidences depend on prior distributions. The priors $r < 0.5$ and $|\alpha_s| < 0.1$ may be regarded as tight ones, while the prior $0.8 < n_s < 1.2$ is often adopted in other studies [38, 43]. More relaxed priors on r and α_s may slightly decrease the Bayes evidences for $M_{n_s r}$ and $M_{n_s \alpha_s}$, which however hardly affects our conclusion.

4.2 HSR parameterization

In Tables 5 we presented the Bayes evidences of models with the HSR parameters, M_ϵ , M_η and $M_{\epsilon\eta}$, as well as their Bayes factors against M_{HZ} . First we reconfirm that the M_{HZ}

^{#6} We do not derive an optimal constraint by averaging over models, as our division of models, M_{n_s} , $M_{n_s r}$ and $M_{n_s \alpha_s}$, is rather artificial, and not strongly based on theoretical motivations.

models	M_{HZ}	M_{n_s}	$M_{n_s r}$	$M_{n_s \alpha_s}$
WMAP5	-1343.1 ± 0.1	-1342.3 ± 0.1	-1343.2 ± 0.1	-1342.8 ± 0.1
		[+0.8 ± 0.2]	[−0.1 ± 0.2]	[+0.3 ± 0.2]
+CMB	-1459.7 ± 0.1	-1458.3 ± 0.1	-1459.2 ± 0.1	-1458.5 ± 0.1
		[+1.4 ± 0.2]	[+0.5 ± 0.2]	[+1.2 ± 0.2]
+BAO	-1345.8 ± 0.1	-1344.1 ± 0.1	-1345.4 ± 0.1	-1344.3 ± 0.1
		[+1.7 ± 0.2]	[+0.4 ± 0.2]	[+1.5 ± 0.2]
+SN	-1499.0 ± 0.1	-1497.4 ± 0.1	-1498.7 ± 0.1	-1497.1 ± 0.1
		[+1.6 ± 0.2]	[+0.3 ± 0.2]	[+1.9 ± 0.2]
+ H_0	-1343.2 ± 0.1	-1342.7 ± 0.1	-1343.4 ± 0.1	-1343.6 ± 0.1
		[+0.5 ± 0.2]	[−0.2 ± 0.2]	[−0.4 ± 0.2]
ALL	-1619.8 ± 0.1	-1615.5 ± 0.1	-1617.2 ± 0.1	-1615.4 ± 0.1
		[+4.3 ± 0.2]	[+2.6 ± 0.2]	[+4.4 ± 0.2]

Table 3: Logarithms of the Bayes evidences for models with standard parameters for the primordial power spectra (upper lows) and their Bayes factors against the reference model M_{HZ} (lower lows, with square brackets).

parameters	M_{n_s}	$M_{n_s r}$	$M_{n_s \alpha_s}$
$\omega_b \times 10^2$	$2.263^{+0.055}_{-0.041}$	$2.278^{+0.051}_{-0.048}$	$2.227^{+0.044}_{-0.059}$
ω_c	$0.1133^{+0.0028}_{-0.0032}$	$0.1128^{+0.0027}_{-0.0033}$	$0.1155^{+0.0032}_{-0.0036}$
$\theta_s \times 10^2$	$104.09^{+0.19}_{-0.24}$	$104.10^{+0.22}_{-0.19}$	$104.12^{+0.21}_{-0.21}$
τ	$0.085^{+0.013}_{-0.017}$	$0.084^{+0.015}_{-0.015}$	$0.095^{+0.015}_{-0.020}$
$\ln[10^{10} A_s]$	$3.137^{+0.028}_{-0.032}$	$3.128^{+0.030}_{-0.035}$	$3.173^{+0.034}_{-0.042}$
n_s	$0.957^{+0.010}_{-0.011}$	$0.962^{+0.012}_{-0.011}$	$0.974^{+0.013}_{-0.015}$
r	—	(0, 0.15)	—
α_s	—	—	$-0.030^{+0.18}_{-0.14}$
n_t	—	(−0.02, 0)	—

Table 4: Constraints for models with standard parameters for the primordial power spectra, M_{n_s} , $M_{n_s r}$ and $M_{n_s \alpha_s}$, from the ALL data set. For bounded parameters, shown are mean values and 68% credible intervals, appearing in subscripts. For unbounded parameters, 95% credible intervals are only shown with parentheses.

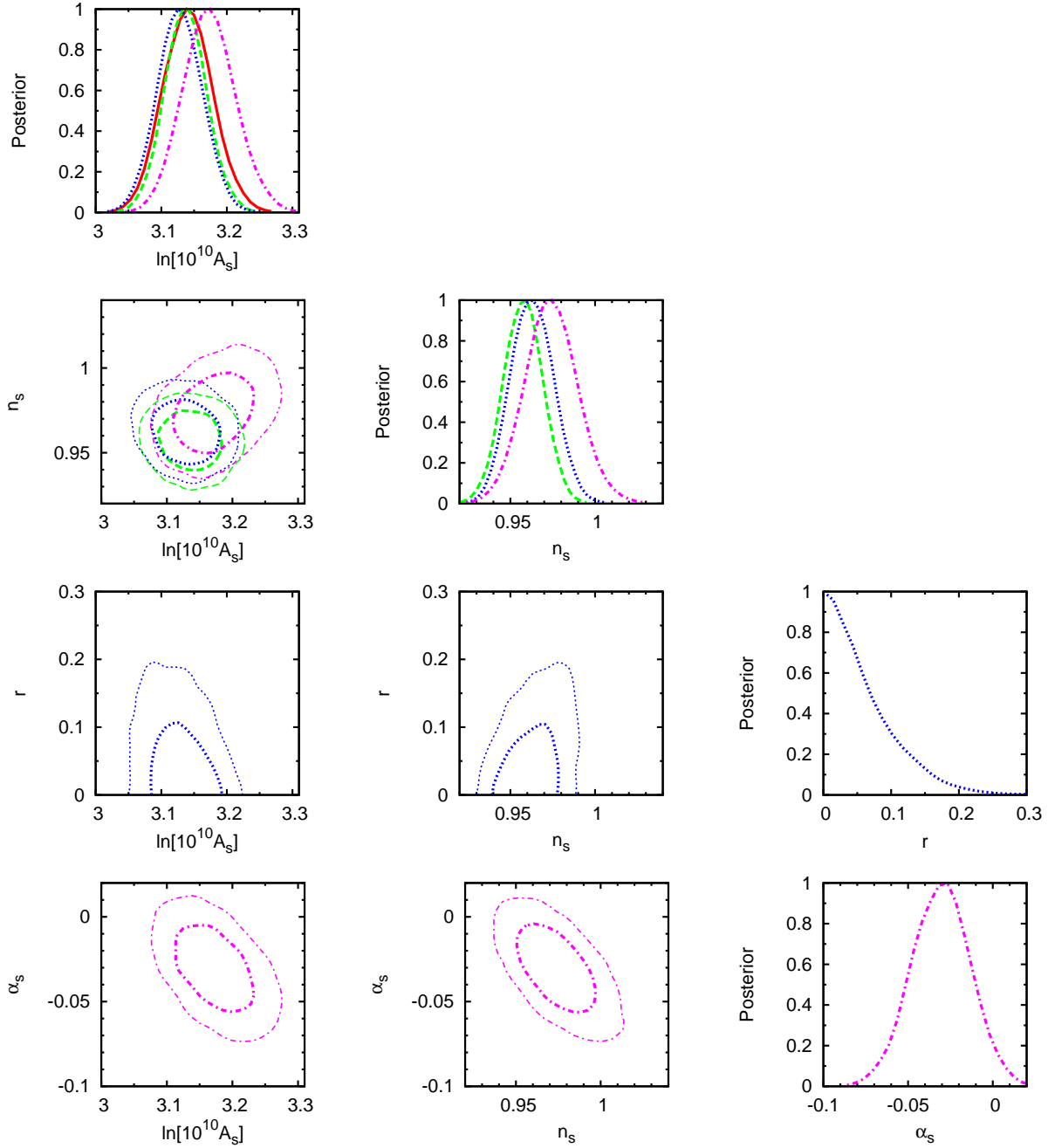


Figure 1: 1d and 2d marginalized posterior distributions of the standard parameters, $\log[10^{10} A_s]$, n_s , r and α_s from the ALL data set. Models shown are M_{n_s} (dashed green line), $M_{n_s r}$ (dotted blue line), $M_{n_s \alpha_s}$ (dot-dashed magenta line) and the reference M_{HZ} (solid red line).

model is negatively supported from the current data. With the ALL data set, the Bayes factors are 5.8, 4.7 and 4.2 for the M_ϵ , M_η and $M_{\epsilon\eta}$ models, respectively. On Jeffreys' scale, these correspond to negative support for the model with the HZ spectrum at decisive or at least strong level. This shows that models of primordial power spectra with inflationary priors can quite well explain the data, that are very poorly fitted by the HZ spectrum.

Let us take a more detailed look at the results so as to look for plausible models of single-field slow-roll inflation from the current data. In Figure 2, we presented the marginalized 1d and 2d posterior distributions for the HSR parameters ϵ_* and η_* . There we explicitly show the parameter region in ϵ_* - η_* plane that are removed by a prior $N > 25$ for $\xi_* = 0$. Also we presented the marginalized posterior distributions for the amplitude of curvature power spectrum A_s and the *derived* standard parameters, n_s , r and α_s , in Figure 3. From Table 5 we consistently observe that the Bayes evidences for M_ϵ are larger than those for M_η and $M_{\epsilon\eta}$, which are nearly equal, for all the data sets we adopted. With the ALL data set, the Bayes factor of M_ϵ against M_η and $M_{\epsilon\eta}$ are 1.1 and 1.6. Thus current data show slight preference for M_ϵ over M_η and $M_{\epsilon\eta}$, which would be significant on Jeffreys' scale.

However, the preference for M_ϵ looks somewhat dependent on several assumptions we adopted in the analysis and the origin is not clear. One possible origin would be the prior $N > 25$, for it eliminates the region $\epsilon_* \gtrsim 0.024$ if $\eta_* = 0$, as can be seen from the shaded region in Figure 2. Thus in the models of M_ϵ , the original top-hat prior $0 < \epsilon_* < 0.1$ is effectively substituted with a top-hat prior $0 < \epsilon_* < 0.024$ due to the prior $N > 25$. As can be seen in the marginal posterior distribution of ϵ_* for M_ϵ in Figure 2, the effective prior region appears to give high likelihood, which results in boosting up the Bayesian evidence for M_ϵ .

Let us examine the origin of preference for M_ϵ in more detail. We have repeated Monte Carlo analyses using the ALL data set, modifying the default setup in several different ways as follows:

- (1) A prior $N > 25$ is removed.
- (2) Contribution from the tensor perturbation is omitted in the power spectra of CMB anisotropies.
- (3) The prior ranges for ϵ_* and η_* are extended from $\epsilon_*, |\eta_*| < 0.1$ to $\epsilon_*, |\eta_*| < 0.2$.
- (4) The higher order HSR parameter ξ_* is included with a top-hat prior $-0.01 < \xi_* < 0.01$.

The results are summarized in Table 6. From the modification (1), we first note that the Bayes evidence for M_ϵ significantly decreases from 5.8 to 4.7 by removal of a prior $N > 25$. The resultant Bayes evidences are very comparable between models M_ϵ and M_η , while more complicated $M_{\epsilon\eta}$ gives a smaller Bayesian evidence.

On the other hand, the largest difference between a model with large ϵ_* (e.g. M_ϵ) and one with small ϵ_* (e.g. M_η) would be generation of the primordial tensor perturbation. Therefore the preference of M_ϵ can also possibly be induced from observably large

contribution of the tensor perturbation in CMB anisotropies. However, this possibility is not supported by the result from the modification (2). The Bayes factor for M_ϵ does not decrease by omission of the tensor contribution in CMB anisotropies, or even comes to increase slightly from 6.0 to 6.3. This is also as expected from the discussions in Section 4.1, where the model $M_{n_s r}$ with nonzero r is less supported, compared with M_{n_s} with vanishing r . From Figure 3 we also note that the running of scalar spectral index for these models is too small to be observed with current data (See also constraints on α_s for $M_{n_s \alpha_s}$ in Figure 1). Therefore the preference for M_ϵ is not from the running of the scalar spectral index either.

With all above demonstrations, we would conclude that the preference for M_ϵ originates from a theoretical prior $N > 25$. Current data is not very constraining enough for us to distinguish models adopted in our analysis and future observations should be waited.

We also examine the dependence of the Bayes evidences on top-hat priors on ϵ_* and η_* . Modification (3) in Table 6 shows that doubling of prior ranges from $\epsilon_*, |\eta_*| < 0.1$ to $\epsilon_*, |\eta_*| < 0.2$ decreases the logarithmic Bayes evidences M_η , $M_{\epsilon\eta}$ by 0.8 and 1.4, respectively. These decrease are almost as expected from the dependence of Bayes evidences on prior ranges, that are about $\ln 2 \simeq 0.7$ and $2 \ln 2 \simeq 1.4$ for M_η and $M_{\epsilon\eta}$, respectively. Contrastively, the Bayes evidence for M_ϵ is unchanged by the modification (3), as the priors $N > 25$ dominates over the original top-hat prior on ϵ_* .

So far we restricted ourselves to models with the HSR parameters up to ϵ and η . Let us examine possible preference for models with higher-order HSR parameters. We have included the third lowest order HSR parameter ξ_* with a top-hat prior $-0.01 < \xi_* < 0.01$ in the modification (4). From Table 6 we observe that the Bayes evidences almost equal or decrease from those with vanishing ξ_* . Therefore current data signify no preference for the models with nonzero ξ_* , and probably models with further higher order HSR parameters, as well. One remark is to be mentioned that above conclusion for models with nonzero ξ_* relies on a prior $N > 25$. As explicitly shown in [23], positive $\xi_* \simeq \mathcal{O}(0.01)$ may be favored when we omit the prior $N > 25$. As we have discussed in Section 2, even for such large ξ_* , a sufficient e-folding number $N > 25$ can possibly be achieved by higher order HSR parameters or other subsequent inflations. However, such complication may make the models less appealing.

The constraints on cosmological parameters for the models with the HSR parameters are presented in Table 7. From the table, we see that constraints on the amplitude and the spectral index of the primordial curvature power spectrum, A_s and n_s , are almost independent of priors on the HSR parameters (See also Figure. 3). Moreover, these constraints are identical with one of Eq. (27-28) from the M_{n_s} models. Therefore we conclude that the optimal constraint we have proposed in Section 4.1 are robust with little dependence on priors from different inflationary models. However, constraints on the tensor perturbations and the running of the spectral index are best dependent on inflationary priors and the presence of neither is suggested from the current data.

models	M_{HZ}	M_ϵ	M_η	$M_{\epsilon\eta}$
WMAP5	-1343.1 ± 0.1	-1341.1 ± 0.1	-1342.2 ± 0.1	-1342.5 ± 0.1
		[+2.0 ± 0.2]	[+0.9 ± 0.2]	[+0.6 ± 0.2]
+CMB	-1459.7 ± 0.1	-1456.8 ± 0.1	-1458.0 ± 0.1	-1458.6 ± 0.1
		[+2.9 ± 0.2]	[+1.7 ± 0.2]	[+1.1 ± 0.2]
+BAO	-1345.8 ± 0.1	-1342.6 ± 0.1	-1343.9 ± 0.1	-1344.2 ± 0.1
		[+3.2 ± 0.2]	[+1.9 ± 0.2]	[+1.6 ± 0.2]
+SN	-1499.0 ± 0.1	-1496.0 ± 0.1	-1497.1 ± 0.1	-1497.3 ± 0.1
		[+3.0 ± 0.2]	[+1.9 ± 0.2]	[+1.7 ± 0.2]
+ H_0	-1343.2 ± 0.1	-1341.4 ± 0.1	-1342.6 ± 0.1	-1342.9 ± 0.1
		[+1.8 ± 0.2]	[+0.6 ± 0.2]	[+0.3 ± 0.2]
ALL	-1619.8 ± 0.1	-1614.0 ± 0.1	-1615.1 ± 0.1	-1615.6 ± 0.1
		[+5.8 ± 0.2]	[+4.7 ± 0.2]	[+4.2 ± 0.2]

Table 5: Logarithms of the Bayes evidences for models with the HSR parameters (upper lows) and their Bayes factors against the reference model M_{HZ} (lower lows, with square brackets).

models	M_{HZ}	M_ϵ	M_η	$M_{\epsilon\eta}$
ALL	-1619.8 ± 0.1	-1614.0 ± 0.1	-1615.1 ± 0.1	-1615.6 ± 0.1
		[+5.8 ± 0.2]	[+4.7 ± 0.2]	[+4.2 ± 0.2]
(1)		-1615.1 ± 0.1	-1615.2 ± 0.1	-1616.1 ± 0.1
		[+4.7 ± 0.2]	[+4.6 ± 0.2]	[+3.7 ± 0.2]
(2)		-1613.9 ± 0.1	-1615.2 ± 0.1	-1615.6 ± 0.1
		[+5.9 ± 0.2]	[+4.6 ± 0.2]	[+4.2 ± 0.2]
(3)		-1614.0 ± 0.1	-1615.9 ± 0.1	-1617.0 ± 0.1
		[+5.8 ± 0.2]	[+3.9 ± 0.2]	[+2.8 ± 0.2]
(4)		-1615.5 ± 0.1	-1614.7 ± 0.1	-1616.2 ± 0.1
		[+4.3 ± 0.2]	[+5.1 ± 0.2]	[+3.6 ± 0.2]

Table 6: Logarithms of the Bayes evidences for models with the HSR parameters (upper lows) and their Bayes factors against the reference model M_{HZ} (lower lows, with square brackets). Several extensions from the default setting are investigated: (1) removal of a prior on e-folding number; (2) omission of the tensor perturbation; (3) imposition of extended top-hat priors, $\epsilon_*, |\eta_*| < 0.2$; (4) inclusion of the third lowest order HSR parameter $-0.01 < \xi_* < 0.01$.

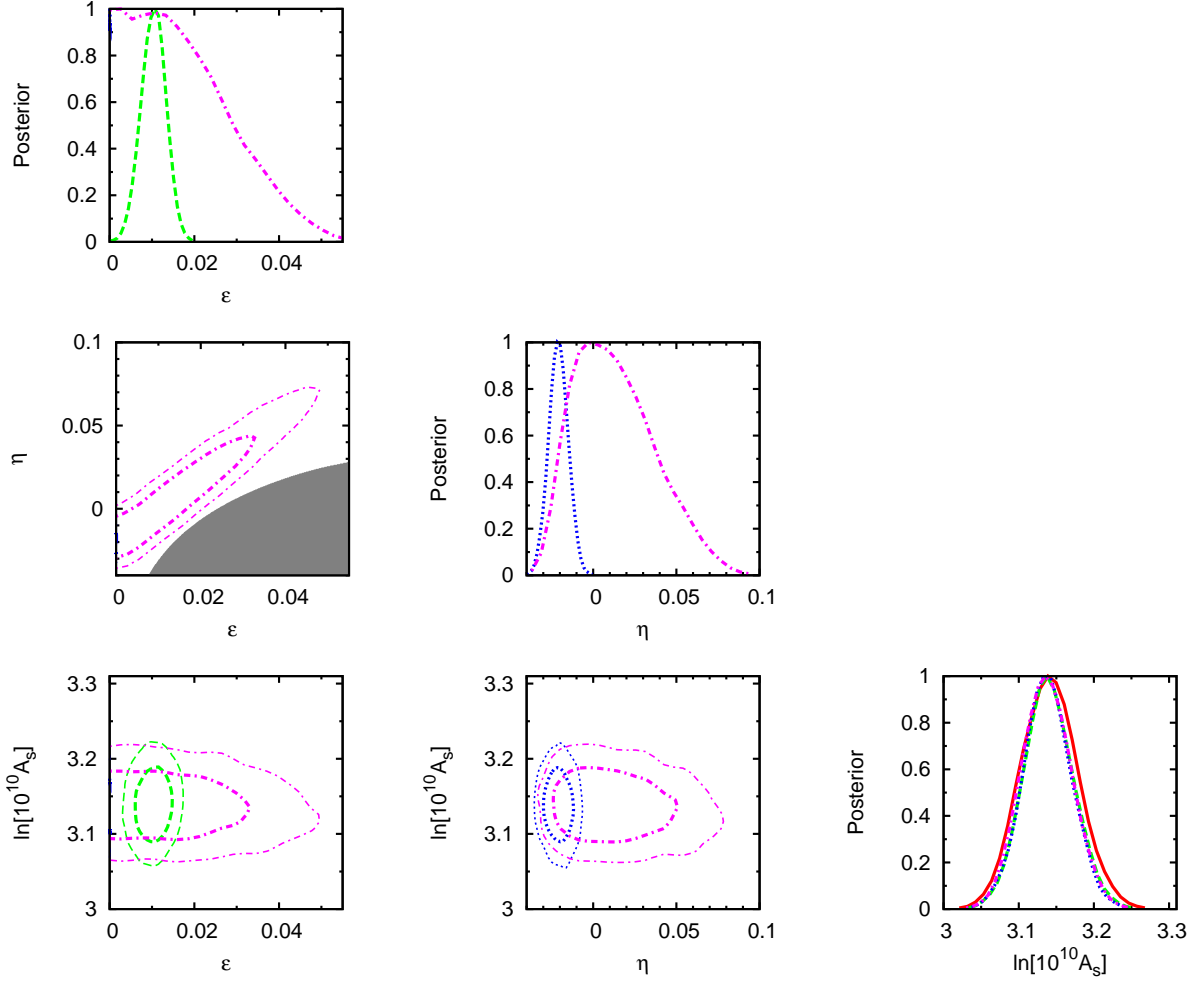


Figure 2: 1d and 2d marginalized posterior distributions for the HSR parameters, ϵ_* and η_* , and the amplitude of the curvature power spectrum $\ln[10^{10} A_s]$. Models shown are M_ϵ (dashed green line), M_η (dotted blue line), $M_{\epsilon\eta}$ (dot-dashed magenta line) and the reference M_{HZ} (solid red line). The gray shaded region is excluded by a prior $N > 25$ when $\xi_* = 0$.

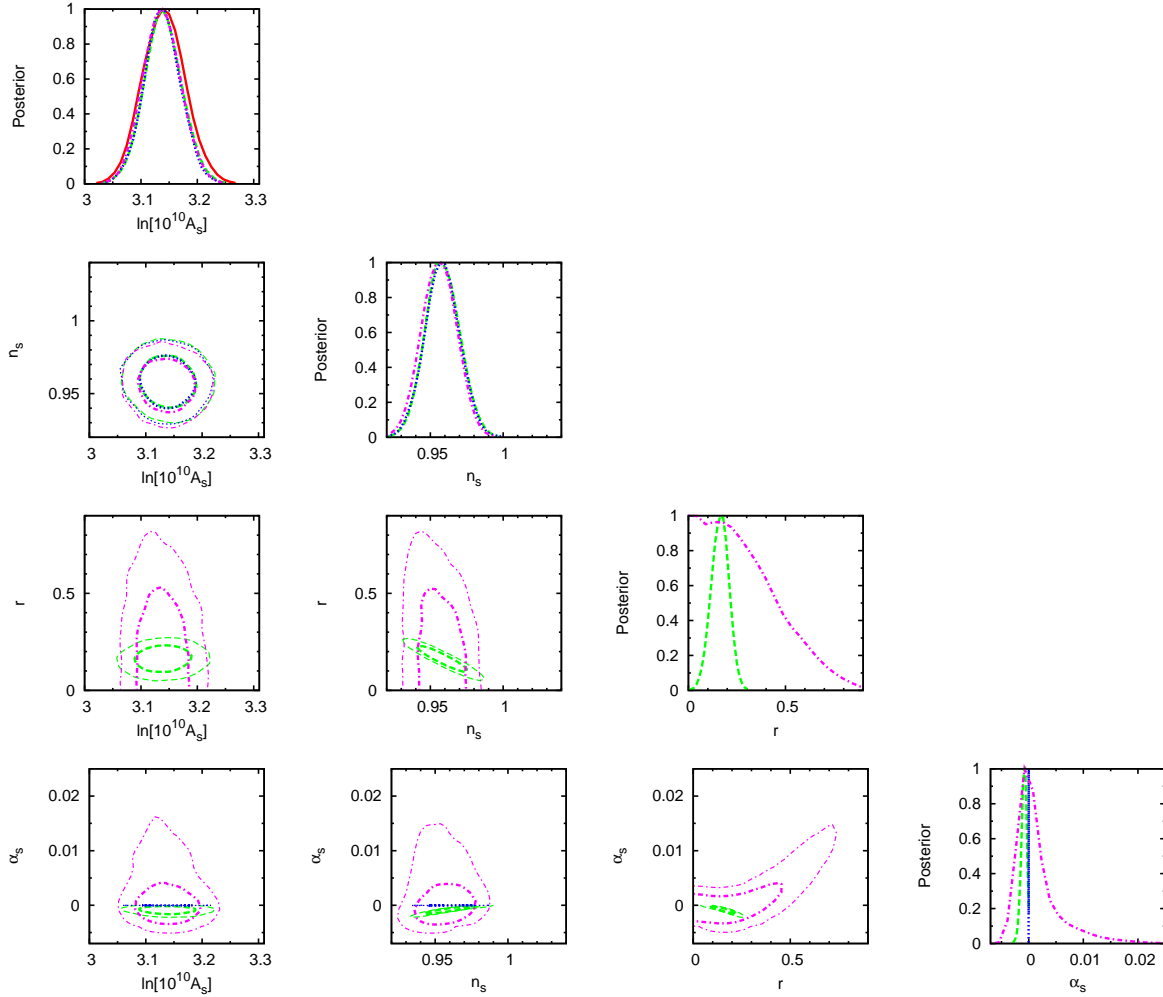


Figure 3: Same figure as in Figure 2 but the posterior distributions for the standard parameters, $\ln[10^{10} A_s]$, n_s , r and α_s , are shown.

parameters	M_ϵ	M_η	$M_{\epsilon\eta}$
$\omega_b \times 10^2$	$2.261^{+0.052}_{-0.048}$	$2.263^{+0.048}_{-0.049}$	$2.260^{+0.051}_{-0.050}$
ω_c	$0.1136^{+0.0031}_{-0.0031}$	$0.1135^{+0.0029}_{-0.0032}$	$0.1134^{+0.0029}_{-0.0032}$
$\theta_s \times 10^2$	$104.12^{+0.22}_{-0.19}$	$104.13^{+0.21}_{-0.20}$	$104.11^{+0.23}_{-0.19}$
τ	$0.086^{+0.013}_{-0.017}$	$0.085^{+0.015}_{-0.014}$	$0.084^{+0.012}_{-0.018}$
ϵ_*	$0.0104^{+0.0028}_{-0.0028}$	—	(0, 0.039)
η_*	—	$-0.0208^{+0.0059}_{-0.0051}$	$0.013^{+0.015}_{-0.030}$
$\ln[10^{10} A_s]$	$3.137^{+0.028}_{-0.032}$	$3.137^{+0.030}_{-0.030}$	$3.137^{+0.027}_{-0.036}$
n_s	$0.958^{+0.011}_{-0.011}$	$0.958^{+0.011}_{-0.010}$	$0.956^{+0.011}_{-0.012}$
r	$0.163^{+0.044}_{-0.043}$	—	(0, 0.64)
$\alpha_s \times 10^3$	$0.92^{+0.57}_{-0.32}$	—	$1.57^{+0.06}_{-3.20}$
$n_t \times 10^2$	$-2.10^{+0.58}_{-0.58}$	—	(-8.1, 0)

Table 7: Constraints for models with the inflationary HSR parameters, M_ϵ , M_η and $M_{\epsilon\eta}$, from the ALL data set. For bounded parameters, shown are mean values and 68% credible intervals, appearing in subscripts. For unbounded parameters, 95% credible intervals are only shown with parentheses.

5 Summary and future outlook

We investigated constraints on the primordial power spectra and comparison of single-field slow-roll inflation models using data from recent observations of CMB combined with measurements of BAO, SN and H_0 . By employing Bayesian model selection, we found that a model with the scale-invariant HZ spectrum is strongly disfavored from current data, in comparison with several simple models allowing scale-dependence of the power spectra. We also proposed an optimal constraint on the primordial power spectra of Eqs. (27-28).

Adopting our somewhat artificial division of models for single-field slow-roll inflation, M_ϵ , M_η and $M_{\epsilon\eta}$ and a theoretical prior $N > 25$, we found preference for these models from current data is almost comparable, but there is a slight but consistent preference for M_ϵ over the others from various data sets. We demonstrated several extension in order to identify the origin of the preference for M_ϵ . A presence of the tensor perturbation is not signified and we found that the preference originates from a prior $N > 25$ which appears to make a prior ranges for ϵ_* center around the region of high likelihood. We also found that slow-roll parameters of higher order are not required from current data. Thus we conclude that while simple models of single-field slow-roll inflation can describe current cosmological observations, data is not enough constraining to distinguish these models we adopted.

Planck [78] and several other ground-based CMB surveys, such as QUIET [79], PolarBear [80], etc. are now under way. In the near future, the tensor to scalar ratio of $r \simeq 0.01$ will be probed with these surveys combined. This allow us to discriminate models of single-field inflation through the prediction on the primordial power spectra or the

slow-roll parameters. Indeed, one of our division of models, M_ϵ will be strongly refused, if the primordial tensor perturbation is not detected by those surveys. Given data from these future surveys, employment of Bayesian model selection would be of great help in several ways, such as constraining cosmological parameters in an optimal way, or assessing a support for a cosmological models statistically.

Acknowledgment

T.S. would like to thank the Japan Society for the Promotion of Science for financial support. This work is supported by Grant-in-Aid for Scientific research from the Ministry of Education, Science, Sports, and Culture (MEXT), Japan, under Contract No. 14102004 (M.K.), and also by World Premier International Research Center Initiative, MEXT, Japan.

References

- [1] A. A. Starobinsky, Phys. Lett. B **91** (1980) 99.
- [2] A. H. Guth, Phys. Rev. D **23**, 347 (1981).
- [3] K. Sato, Mon. Not. Roy. Astron. Soc. **195**, 467 (1981).
- [4] A. D. Linde, Phys. Lett. B **108**, 389 (1982).
- [5] A. J. Albrecht and P. J. Steinhardt, Phys. Rev. Lett. **48**, 1220 (1982).
- [6] A. A. Starobinsky, JETP Lett. **30** (1979) 682 [Pisma Zh. Eksp. Teor. Fiz. **30** (1979) 719].
- [7] V. F. Mukhanov and G. V. Chibisov, JETP Lett. **33** (1981) 532 [Pisma Zh. Eksp. Teor. Fiz. **33** (1981) 549].
- [8] S. W. Hawking, Phys. Lett. B **115**, 295 (1982).
- [9] A. A. Starobinsky, Phys. Lett. B **117** (1982) 175.
- [10] A. H. Guth and S. Y. Pi, Phys. Rev. Lett. **49**, 1110 (1982).
- [11] A. D. Linde, Phys. Lett. B **116**, 335 (1982).
- [12] J. M. Bardeen, P. J. Steinhardt and M. S. Turner, Phys. Rev. D **28**, 679 (1983).
- [13] L. F. Abbott and M. B. Wise, Nucl. Phys. B **244**, 541 (1984).

- [14] E. J. Copeland, E. W. Kolb, A. R. Liddle and J. E. Lidsey, Phys. Rev. D **48**, 2529 (1993) [arXiv:hep-ph/9303288].
- [15] J. E. Lidsey, A. R. Liddle, E. W. Kolb, E. J. Copeland, T. Barreiro and M. Abney, Rev. Mod. Phys. **69**, 373 (1997) [arXiv:astro-ph/9508078].
- [16] S. M. Leach and A. R. Liddle, Mon. Not. Roy. Astron. Soc. **341**, 1151 (2003) [arXiv:astro-ph/0207213].
- [17] R. Easther and W. H. Kinney, Phys. Rev. D **67**, 043511 (2003) [arXiv:astro-ph/0210345].
- [18] W. H. Kinney, E. W. Kolb, A. Melchiorri and A. Riotto, Phys. Rev. D **69**, 103516 (2004) [arXiv:hep-ph/0305130].
- [19] S. M. Leach and A. R. Liddle, Phys. Rev. D **68**, 123508 (2003) [arXiv:astro-ph/0306305].
- [20] H. Peiris and R. Easther, JCAP **0607**, 002 (2006) [arXiv:astro-ph/0603587].
- [21] W. H. Kinney, E. W. Kolb, A. Melchiorri and A. Riotto, Phys. Rev. D **74**, 023502 (2006) [arXiv:astro-ph/0605338].
- [22] J. Martin and C. Ringeval, JCAP **0608**, 009 (2006) [arXiv:astro-ph/0605367].
- [23] H. Peiris and R. Easther, JCAP **0610**, 017 (2006) [arXiv:astro-ph/0609003].
- [24] J. Lesgourgues and W. Valkenburg, Phys. Rev. D **75**, 123519 (2007) [arXiv:astro-ph/0703625].
- [25] B. A. Powell and W. H. Kinney, JCAP **0708**, 006 (2007) [arXiv:0706.1982 [astro-ph]].
- [26] J. Lesgourgues, A. A. Starobinsky and W. Valkenburg, JCAP **0801**, 010 (2008) [arXiv:0710.1630 [astro-ph]].
- [27] R. Bean, D. J. H. Chung and G. Geshnizjani, Phys. Rev. D **78**, 023517 (2008) [arXiv:0801.0742 [astro-ph]].
- [28] J. Hamann, J. Lesgourgues and W. Valkenburg, JCAP **0804**, 016 (2008) [arXiv:0802.0505 [astro-ph]].
- [29] P. Adshead and R. Easther, JCAP **0810**, 047 (2008) [arXiv:0802.3898 [astro-ph]].
- [30] N. Agarwal and R. Bean, Phys. Rev. D **79**, 023503 (2009) [arXiv:0809.2798 [astro-ph]].
- [31] B. A. Powell, K. Tzirakis and W. H. Kinney, JCAP **0904**, 019 (2009) [arXiv:0812.1797 [astro-ph]].

- [32] E. Komatsu *et al.* [WMAP Collaboration], *Astrophys. J. Suppl.* **180**, 330 (2009) [arXiv:0803.0547 [astro-ph]].
- [33] A. Slosar *et al.*, *Mon. Not. Roy. Astron. Soc.* **341**, L29 (2003) [arXiv:astro-ph/0212497].
- [34] M. Beltran, J. Garcia-Bellido, J. Lesgourgues, A. R. Liddle and A. Slosar, *Phys. Rev. D* **71**, 063532 (2005) [arXiv:astro-ph/0501477].
- [35] R. Trotta, *Mon. Not. Roy. Astron. Soc.* **378**, 72 (2007) [arXiv:astro-ph/0504022].
- [36] M. Bridges, A. N. Lasenby and M. P. Hobson, *Mon. Not. Roy. Astron. Soc.* **369**, 1123 (2006) [arXiv:astro-ph/0511573].
- [37] M. Kunz, R. Trotta and D. Parkinson, *Phys. Rev. D* **74**, 023503 (2006) [arXiv:astro-ph/0602378].
- [38] D. Parkinson, P. Mukherjee and A. R. Liddle, *Phys. Rev. D* **73**, 123523 (2006) [arXiv:astro-ph/0605003].
- [39] M. Bridges, A. N. Lasenby and M. P. Hobson, arXiv:astro-ph/0607404.
- [40] C. Pahud, A. R. Liddle, P. Mukherjee and D. Parkinson, *Phys. Rev. D* **73**, 123524 (2006) [arXiv:astro-ph/0605004].
- [41] A. R. Liddle, P. Mukherjee and D. Parkinson, arXiv:astro-ph/0608184.
- [42] A. F. Heavens, T. D. Kitching and L. Verde, *Mon. Not. Roy. Astron. Soc.* **380**, 1029 (2007) [arXiv:astro-ph/0703191].
- [43] C. Gordon and R. Trotta, *Mon. Not. Roy. Astron. Soc.* **382**, 1859 (2007) [arXiv:0706.3014 [astro-ph]].
- [44] P. Mukherjee and A. R. Liddle, arXiv:0803.1738 [astro-ph].
- [45] R. Trotta, *Contemp. Phys.* **49**, 71 (2008) [arXiv:0803.4089 [astro-ph]].
- [46] P. Mukherjee and D. Parkinson, *Int. J. Mod. Phys. A* **23** (2008) 787.
- [47] M. Bridges, F. Feroz, M. P. Hobson and A. N. Lasenby, arXiv:0812.3541 [astro-ph].
- [48] A. R. Liddle, arXiv:0903.4210 [hep-th].
- [49] I. Sollom, A. Challinor and M. P. Hobson, *Phys. Rev. D* **79**, 123521 (2009) [arXiv:0903.5257 [astro-ph.CO]].
- [50] K. Ichikawa, M. Kawasaki, K. Nakayama, T. Sekiguchi and T. Takahashi, *JCAP* **0908**, 013 (2009) [arXiv:0905.2237 [astro-ph.CO]].

- [51] J. Valiviita and T. Giannantonio, arXiv:0909.5190 [astro-ph.CO].
- [52] D. Baumann *et al.* [CMBPol Study Team Collaboration], AIP Conf. Proc. **1141**, 10 (2009) [arXiv:0811.3919 [astro-ph]].
- [53] S. M. Leach, A. R. Liddle, J. Martin and D. J. Schwarz, Phys. Rev. D **66**, 023515 (2002) [arXiv:astro-ph/0202094].
- [54] M. B. Hoffman and M. S. Turner, Phys. Rev. D **64**, 023506 (2001) [arXiv:astro-ph/0006321].
- [55] W. H. Kinney, Phys. Rev. D **66**, 083508 (2002) [arXiv:astro-ph/0206032].
- [56] A. R. Liddle, Phys. Rev. D **68**, 103504 (2003) [arXiv:astro-ph/0307286].
- [57] E. D. Stewart and D. H. Lyth, Phys. Lett. B **302**, 171 (1993) [arXiv:gr-qc/9302019].
- [58] M. Cortes, A. R. Liddle and P. Mukherjee, Phys. Rev. D **75**, 083520 (2007) [arXiv:astro-ph/0702170].
- [59] A. Kosowsky, M. Milosavljevic and R. Jimenez, Phys. Rev. D **66**, 063007 (2002) [arXiv:astro-ph/0206014].
- [60] E. Komatsu and U. Seljak, Mon. Not. Roy. Astron. Soc. **336**, 1256 (2002) [arXiv:astro-ph/0205468].
- [61] J. Dunkley *et al.* [WMAP Collaboration], Astrophys. J. Suppl. **180**, 306 (2009) [arXiv:0803.0586 [astro-ph]].
- [62] M. R. Nolta *et al.* [WMAP Collaboration], Astrophys. J. Suppl. **180**, 296 (2009) [arXiv:0803.0593 [astro-ph]].
- [63] G. Hinshaw *et al.* [WMAP Collaboration], Astrophys. J. Suppl. **180**, 225 (2009) [arXiv:0803.0732 [astro-ph]].
- [64] C. L. Reichardt *et al.*, arXiv:0801.1491 [astro-ph].
- [65] J. L. Sievers *et al.*, Astrophys. J. **660**, 976 (2007) [arXiv:astro-ph/0509203].
- [66] W. C. Jones *et al.*, Astrophys. J. **647**, 823 (2006) [arXiv:astro-ph/0507494].
- [67] F. Piacentini *et al.*, Astrophys. J. **647**, 833 (2006) [arXiv:astro-ph/0507507].
- [68] T. E. Montroy *et al.*, Astrophys. J. **647**, 813 (2006) [arXiv:astro-ph/0507514].
- [69] R. B. Friedman *et al.* [QUaD collaboration], arXiv:0901.4334 [astro-ph.CO].
- [70] B. A. Reid *et al.*, arXiv:0907.1659 [astro-ph.CO].

- [71] M. Kowalski *et al.* [Supernova Cosmology Project Collaboration], *Astrophys. J.* **686**, 749 (2008) [arXiv:0804.4142 [astro-ph]].
- [72] W. J. Percival *et al.*, arXiv:0907.1660 [astro-ph.CO].
- [73] A. G. Riess *et al.*, arXiv:0905.0695 [astro-ph.CO].
- [74] F. Feroz, M. P. Hobson and M. Bridges, arXiv:0809.3437 [astro-ph].
- [75] A. Lewis and S. Bridle, *Phys. Rev. D* **66**, 103511 (2002) [arXiv:astro-ph/0205436].
- [76] Skilling J., 2004, AIP Conference Proceedings of the 24th International Workshop on Bayesian Inference and Maximum Entropy Methods in Science and Engineering, Vol. 735, pp. 395-405
- [77] P. Mukherjee, D. Parkinson and A. R. Liddle, *Astrophys. J.* **638**, L51 (2006) [arXiv:astro-ph/0508461].
- [78] [Planck Collaboration], arXiv:astro-ph/0604069.
- [79] D. Samtleben and f. t. Q. Collaboration, *Nuovo Cim.* **122B**, 1353 (2007) [arXiv:0802.2657 [astro-ph]].
- [80] <http://bolo.berkeley.edu/polarbear/>